


Article

Characterization of HCN-Derived Thermal Polymer: Implications for Chemical Evolution

Saúl A. Villafaña-Barajas ¹, Marta Ruiz-Bermejo ², Pedro Rayo-Pizarroso ² and María Colín-García ^{3,*} 

¹ Posgrado en Ciencias de la Tierra, Universidad Nacional Autónoma de México, Ciudad Universitaria, Cd. Mx 04510, Mexico; saulvillafanephd@gmail.com

² Centro de Astrobiología (CSIC-INTA), Dpto. Evolución Molecular, Ctra. Torrejón-Ajalvir, km 4, Torrejón de Ardoz, 28850 Madrid, Spain; ruizbm@cab.inta-csic.es (M.R.-B.); prayo@cab.inta-csic.es (P.R.-P.)

³ Instituto de Geología, Universidad Nacional Autónoma de México, Ciudad Universitaria, Cd. Mx 04510, Mexico

* Correspondence: mcolin@geologia.unam.mx; Tel.: +52-(55)-56224300-164

Received: 28 June 2020; Accepted: 4 August 2020; Published: 11 August 2020



Abstract: Hydrogen cyanide (HCN)-derived polymers have been recognized as sources of relevant organic molecules in prebiotic chemistry and material sciences. However, there are considerable gaps in the knowledge regarding the polymeric nature, the physicochemical properties, and the chemical pathways along polymer synthesis. HCN might have played an important role in prebiotic hydrothermal environments; however, only few experiments use cyanide species considering hydrothermal conditions. In this work, we synthesized an HCN-derived thermal polymer simulating an alkaline hydrothermal environment (i.e., HCN (l) 0.15 M, 50 h, 100 °C, pH approximately 10) and characterized its chemical structure, thermal behavior, and the hydrolysis effect. Elemental analysis and infrared spectroscopy suggest an important oxidation degree. The thermal behavior indicates that the polymer is more stable compared to other HCN-derived polymers. The mass spectrometric thermal analysis showed the gradual release of several volatile compounds along different thermal steps. The results suggest a complicate macrostructure formed by amide and hydroxyl groups, which are joined to the main reticular chain with conjugated bonds (C=O, N=O, –O–C=N). The hydrolysis treatment showed the pH conditions for the releasing of organics. The study of the synthesis of HCN-derived thermal polymers under feasible primitive hydrothermal conditions is relevant for considering hydrothermal vents as niches of chemical evolution on early Earth.

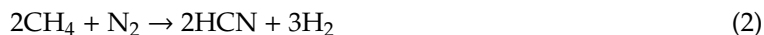
Keywords: HCN-derived thermal polymer; thermolysis; alkaline hydrothermal systems; chemical evolution

1. Introduction

Hydrogen cyanide, HCN, has been considered as a paramount raw material to reach high chemical complexity in the field of prebiotic chemistry and chemical evolution [1–4]. HCN could have been formed from different endogenic sources, on early Earth [3,5–9], or it could be formed exogenically and then carried to Earth [4,10–12].

The concentration of HCN on primitive environments is still discussed. Some authors argue that it must be low (10^{-10} – 10^{-13} mol L⁻¹; [13,14]); recently, Fábíán et al. [15] proposed the formation of floating HCN patches with a >1 mol L⁻¹ concentration. In addition, Holm and Neubeck [5] suggested that HCN could have been produced under hydrothermal conditions from CH₄, NH₃, and other dissolved species (i.e., N₂, CO). The main reactions are as follows:





It is well known that HCN solutions spontaneously polymerize [16]. During the polymerization of HCN, an insoluble black polymer is formed under different synthesis conditions [17,18]. After hydrolysis treatments, these complex polymers release an important number of organic molecules [2,17,19–21]; recently, their applications on material sciences have been studied [22–25]. It has been demonstrated that the possible chemical structure and the thermal properties of these polymers directly depend on the conditions of the synthesis (e.g., raw material, temperature, concentration, reaction time, and atmosphere). Therefore, the HCN-derived polymers should be considered as a family of complex substances [18,26].

The synthesis of these complex materials has been dominated by the use of cyanide salts (e.g., sodium, potassium, and ammonia salts) dissolved in aqueous medium in a broad range of temperatures (from -20 up to 100 °C) at alkaline conditions ($\text{pH} > 8$) (e.g., [18,26–28]). Other experiments have synthesized HCN-derived polymers by heating formamide [29,30], aminomalononitrile, AMN, [24] and diaminomaleonitrile, DAMN [18].

There is robust information about the mechanisms and chemical conditions that lead to the formation of DAMN from HCN, cyanide (CN^-), and intermediate species, such as AMN [31–34]. There are also some proposals about their polymeric structure [18,20,28,35–39]. However, the pathways for the formation of HCN-derived polymers remain unsolved; new approaches suggest that hydrolysis/oxidation reactions along polymerization directly affect the physicochemical properties of these materials [26,28].

HCN polymers might have had an important role in chemical evolution; nonetheless, there are several inconsistencies regarding the initial concentration of HCN and the primitive scenario where polymers could have been formed [4,13,14]. It has been proposed that HCN could have experienced important reactions in prebiotic hydrothermal environments, and it could be an essential part of the stepwise series to produce successively more complex organic molecules [5,40–46]. Nonetheless, only a few research studies have used cyanide species in hydrothermal experiments [47–49] (for more details, see Aubrey et al., 2009 [46]).

There is a growing interest in the chemistry of HCN solutions in prebiotic chemistry studies. In addition, alkaline environments are shown to be very relevant for studies related to the origin of life [50,51]. However, the synthesis of HCN polymers under simulated hydrothermal conditions has been scarcely explored. In a recent paper [52], we studied the thermolysis of HCN under simulating HV conditions; along with the identification of formed products in solution in this experiment, we also detected the formation a black polymer. Hence, as we are interested in a systematic study of HCN under HV conditions, an HCN-derived thermal polymer (HCN-DTP) from a hydrogen cyanide solution was synthesized and characterized in detail in order to better constrain the properties of these fascinating substances. For characterization, we used a method previously developed for the analysis and systematic characterization of HCN-derived polymers that consisted of elemental analysis, infrared spectroscopy (IR), thermogravimetric (TG) and mass spectrometric thermal analysis (TG-MS), hydrolysis treatment, and GC-MS analysis, in order to gain information about its structure, nature, thermal behavior, and to evaluate its role as a precursor of organic molecules [17,18,26–28,53–55]. This comprehensive analytical study shows the identification of single biomolecules of interest in the chemical evolution research but also gives clues about the complex nature of the macrostructure of the HCN-DTP. It is necessary to know the relationships among the synthesis conditions, the structure, and the properties of the HCN polymers, in order to increase our knowledge about the possible role of HCN polymerization in prebiotic chemistry. These would lead to the generation of polymeric structures with potential properties fit for new or secondary reactions in unexplored prebiotic scenarios. In addition, these polymers would have potential applications in material sciences [18]. Interestingly, the HCN-DTP here described presents characteristics not previously reported.

2. Materials and Methods

Production of HCN. HCN solution (0.15 M) was produced in situ by the reaction between KCN and H₂SO₄. HCN gas was dissolved into Milli Q water under an argon atmosphere. The concentration of HCN was determined by titration with an aqueous solution of AgNO₃ [56]. The reaction for producing HCN is not scalable and must be carried out with many precautions due to the high toxicity of HCN. Although the concentration of HCN solution (0.15 M) could be higher than the feasible concentration on primitive environments, it was chosen according to previous reports that consider it as a practical and a consistent concentration for the polymerization of HCN [57].

After synthesis, the pH of the HCN solution was adjusted to approximately 10 by adding drops (approximately 10 µL) of a concentrated KOH solution (0.1 M) until the desired pH was reached; this was done to have an important amount of free cyanide in solution, thus avoiding a high potassium concentration. It has been observed that the formation of HCN polymers is favored in alkaline media [18], and we wanted to induce the formation of the polymer and prevent its hydrolysis.

Synthesis of HCN-derived thermal polymer. Experiments were carried out in a static system at 100 °C. Aliquots of the HCN solution (0.15 M, 5 mL) were placed in glass tubes and heated for 50 h. After the thermolysis treatment, the sample was cooled at room temperature. Then, it was possible to identify two different fractions: a soluble fraction (brown yellow) and a black viscous fraction, the HCN-DTP. HCN-DTP (black fraction) was separated from the rest of the soluble fraction (yellow) by centrifugation (10 min, 15 °C, 23,000 rpm). The procedure was carried out four times in order to have a considerable amount of the material (approximately 50 mg), since the yield of the polymer is low [18,26]. The reaction temperature and the pH were both chosen considering conditions surrounding alkaline hydrothermal environments [58]. In addition, this temperature was selected to synthesize organic molecules, and to favor the polymerization reactions of HCN, cyanide salts, and DAMN (for more details, see reference [2]). In contrast with previous reports [2,29,47,59], HCN-DTP does not form appreciable solid particles, although it was prepared above the concentration that favors polymerization reaction (>0.01 M) [14,31]. Recently, Ruiz-Bermejo and co-workers [18,26] have proved that high temperatures and low concentrations of raw material (i.e., up to 90 °C and <1 M) resulted in a low yield of the polymer. According to this, the nature of HCN-DTP is the result of the domain of hydrolysis/oxidation reactions over polymerization during thermolysis (see below). Therefore, the common insoluble black HCN polymers [17] do not have the same nature that the HCN-DTP produced in this experiment. Finally, the fractions were freeze-dried under reduced pressure, resulting in two fractions: a yellow oily precipitate and a black solid powder (HCN-DTP). In this report, different analyses were carried out with the black solid powder.

Elemental analysis. The content of C, N, H, and oxygen was measured. The HCN-derived thermal polymer was examined for the determination of the mass fractions of carbon, hydrogen, and nitrogen (in percentage with respect to weight) in a PerkinElmer® Elemental Analyzer, model CNHS-2400. The percentage of oxygen of the sample was calculated by difference.

FT-IR spectroscopy. Spectra were obtained with a FT-IR spectrometer (Nicolet®, model NEXUS 67) configured with a DRIFT reflectance accessory (Harrick, model Praying Mantis DRP). The spectra were obtained in CsI pellets in the 4000–450 cm⁻¹ spectral region, with a spectral resolution of 2 cm⁻¹.

Thermal analysis. Thermogravimetry (TG), differential thermal analysis (DTG), and differential scanning calorimetry (DSC) measurements were performed in a simultaneous thermal analyzer model SDTQ-600/Thermo Star from TA Instruments®. Thermal analysis was performed in an isothermal mode for 20 min; then, a heating ramp of 10 °C/min was programmed until 1000 °C under an argon atmosphere (100 mL/min). A coupled TG-MS system using an electron-impact quadrupole mass-selective detector (model Thermostat QMS200 M3) was used to analyze the main species during the dynamic thermal decomposition of the fragmentation processes of the sample.

Hydrolysis. HCN-DTP was hydrolyzed using the method developed by Ferris [19] that consisted of an acid hydrolysis followed by a basic hydrolysis. The conditions for acid hydrolysis were HCl 6N/100–110 °C/16–24 h; for basic hydrolysis, they were NaOH 0.1 N/100 °C/6 h. After treatment,

the product was analyzed by GC-MS in a 6859 network GC system coupled to a 5975 VL MSD with triple-axis detector operating in the electron-impact (EI) mode at 70 eV (Agilent®); an HP-5 MS column (30 m × 0.25 mm i.d. × 0.25 μm film thickness) was used; the analysis was carried out using the derivatization method and the GC oven program developed by Marin-Yaseli [60] to detect polar organic compounds. When available, the identified compounds were confirmed against authentic standard mass spectra and retention times. Other organic compounds were identified by searching their mass spectra in the NIST (The National Institute of Standards and Technology) database. For identification purposes, we considered only peaks with a signal-to-noise ratio over 10. Those peaks whose match probability in the database were below 90%, and/or those that were tentatively or ambiguously identified were considered unidentified and are not discussed in this paper.

3. Results

3.1. Elemental Analysis

Elemental analysis shows that the synthesized polymer (HCN-DTP) is compositionally different from other HCN-derived polymers; it is highly oxidized. The elemental composition of HCN-DTP, in percentage, was C 23.2%, H 3.1%, N 19.9%, and O 53.8%. The oxygen concentration (%) was calculated by subtraction of the experimental elemental analysis data. When these results are compared to other syntheses under analogous conditions (i.e., cyanide source, alkaline aqueous solution, [>0.1], >25 °C, free oxygen) (Table S1), it is evident that the content of hydrogen is very similar. However, values of carbon and nitrogen are almost half that reported. This depletion is counteracted by the considerably higher content of oxygen in our sample compared with the values founded in analogous experiments [18,26–28,54]. Even, at similar initial concentrations and high temperatures in other experiments (i.e., 0.1 M NH₄CN, 80 °C during 96 h), only the hydrogen content is similar to our results (e.g., C 38–40%; N 37–39%; H 3–4%; O 16–20%) (Table S1). The depletion of nitrogen can be related to the effect of high temperatures, which increase denitrogenation, hydrolysis, and oxidation processes, throughout polymerization; this process results in oxidized macrostructures [26]. In addition, previous experiments that used net HCN [e.g., DuPont (E.I. Du Pont de Nemours & Co., Inc., Wilmington, DE, USA) HCN_(g) + H₂O_(l) and HCN_(l) + NH_{3(aq)} 0 °C, 4 days] did not show similar trends. The higher oxygen value reported in other experiments is around 25%; it has been associated with a long-time reaction (i.e., one month) and different synthesis and storage conditions [27].

The oxygen content could depend on the polymerization conditions, such as the presence of ammonium in the reaction medium, the temperature, the reaction time, and the raw material [26,28]. In addition, HCN-derived polymers are hygroscopic, and they can absorb a considerable amount of water from air moisture [18]. In fact, thermograms suggest that our sample retains around approximately 10% of H₂O (peak at 55 °C in the DTG curve, see below), and furthermore, the real amount of structural oxygen is around 43.8%. Even considering these contributions, the oxygen content is unexpectedly high. Hence, other mechanisms should be related to the oxidation of the polymer, such as hydrolysis and oxidation reactions [3,26,36].

The molar ratios calculated for HCN-DTP were C/N 1.36; H/N 2.18; O/N 1.93. This suggests that our polymer contains about approximately 2 atoms of oxygen and 2 atoms of hydrogen per nitrogen. The molecular formula proposed is C₁₅H₂₄N₁₁O₂₁. This indicates that our HCN-DTP polymer has a great amount of oxygenated functional groups in the polymeric structure, and it differs from other already studied HCN polymers. In order to identify these functional groups, a Fourier transform infrared (FT-IR) study was performed.

3.2. Fourier Transform Infrared (FT-IR) Spectroscopy

The IR-light exposition generates a complex band-pattern for HCN-DTP; those bands can be associated with functional groups. Although IR spectra provide important information about the functional groups that constitute these polymers, there is not enough information to associate a

spectrum with a specific synthesis method. The IR reflectance spectra of HCN-derived polymers prepared under diverse experimental conditions (Table S1 Supplementary Information) show similar bands [17,18,26,27,61] to the bands identified in our polymer.

Figure 1 shows the IR spectrum of HCN-DTP. As in previous reports, the FT-IR spectra are divided into four main regions: region I (3700–3000 cm^{-1}), region II (2275–2000 cm^{-1}), region III (1825–1000 cm^{-1}), and region VI (centered at 660 cm^{-1}) [26] (Figure 1). Region I can be assigned mainly to N-containing groups of primary and secondary amines (3338 cm^{-1} , –NH asymmetric stretch; 3211 cm^{-1} , –NH₂ symmetric stretch). In addition, OH groups of carboxylic acids and/or methyl groups in aliphatic compounds (2964 cm^{-1} ; OH stretch, –CH₃ asymmetric and symmetric stretch) may overlap. Markedly, the bands at 2798 and 2713 cm^{-1} have not been reported before. These bands are associated with CH₃ symmetric stretch and attached with aromatic groups and/or nitrogen and oxygen atoms [62].

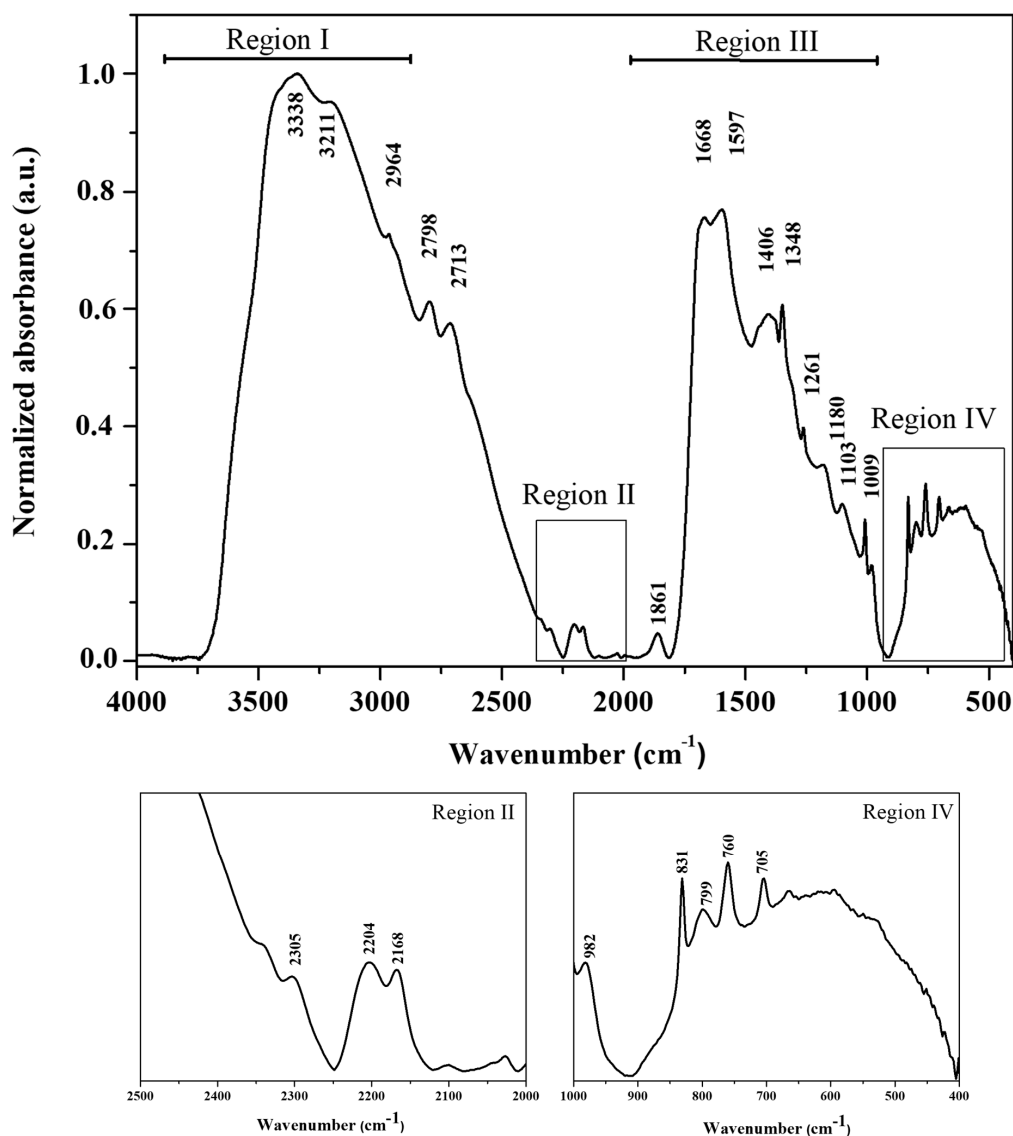


Figure 1. Fourier transform infrared (FT-IR) spectrum of hydrogen cyanide (HCN)-derived thermal polymer. Four regions can be recognized; the band assignments are given in the text and summarized in Table S2.

Region II is characteristic of nitrile groups. In general, three well-defined absorption bands are displayed in this region (at 2305, 2204, and 2168 cm^{-1}); their intensity and position vary depending on synthesis conditions [27]. The first band is associated with isocyanates groups (NCO asymmetric

stretch), while the band at 2204 cm^{-1} may be related with azides and or cyanamides ($\text{N}=\text{N}=\text{N}$ asymmetric stretch, $-\text{C}=\text{N}$ stretch). Some authors have reported a clear band at 2200 cm^{-1} due to $\text{C}\equiv\text{N}$ stretching on HCN polymers formed from formamide [29,30]. However, the possible interaction among bonds such as $\text{X}\equiv\text{Y}$ and $\text{X}=\text{Y}=\text{Z}$ (where X, Y, and Z can be carbon, oxygen, or nitrogen atoms) must be considered. The band at 2168 cm^{-1} is related to the same functional groups, such as carbodiimide groups [17]. In addition, there are appreciable bands around 2340, 2100, and 2026 cm^{-1} .

The third spectral region displays several bands with well-resolved peaks. The band at 1861 cm^{-1} can be associated to carbonyl compounds ($\text{C}=\text{O}$ stretch). Additionally, bands at 1668 and 1597 cm^{-1} may correspond to overtones, and a combination of esters, ketones, amides, and carboxylic acids functional groups. The presence of these bands can be related with hydrolysis at high temperatures, and/or oxidation reactions that yield oxygenated groups [18]. Moreover, the IR spectrum exhibits bands that may correspond to $-\text{CH}_3$ and $-\text{CH}_2$ in unsaturated or cyclic compounds (1406 and 1348 cm^{-1}) associated with adjacent electronegative atoms, such as nitrogen and oxygen (e.g., CH_3 , CH_2 asymmetric/symmetric stretching, wagging and bending vibrations, NO_2 symmetric stretch, NCO symmetric stretch, $\text{H}-\text{C}-\text{H}$ bending). Previous reports [18] have proposed that the absorption bands in this region can be associated with amide bonds and/or heteroaromatic or heterocyclic groups. Likewise, the peak at 1261 cm^{-1} could be linked with amide bonds, esters, or amines. The last relevant signals (Region IV) could be associated with $-\text{CH}_3$ and $-\text{CH}_2$ groups and/or $\text{C}-\text{C}$ stretch with no H on central carbon in straight and branched chains (1180 , 1103 , and 1009 cm^{-1}), and aliphatic insaturation and/or substituted aromatics (982 , 831 , 799 , 760 , and 705 cm^{-1}) [62].

New kinetic studies, considering the polymerization of aqueous solutions of NH_4CN at different temperatures, showed that the shape and width of the bands at approximately 3340 and 1645 cm^{-1} can be interpreted as a highly conjugated macrostructure, and that it could be related with the presence of oxygenated functional groups (i.e., $-\text{COOH}$ and $-\text{CONH}_2$) at $90\text{ }^\circ\text{C}$ [26]. In our case, the band in Region I is centered at 3338 cm^{-1} , while the band at 1645 cm^{-1} is divided in two well-defined peaks (1668 and 1597 cm^{-1}) (see above).

Therefore, the elemental analysis and the infrared spectra analysis suggest that HCN-DTP shows a higher degree of hydrolysis and/or oxidation than other polymers (Table S1). The structure of this polymer can be composed by a greater number of conjugated bonds [e.g., $\text{C}=\text{C}$, $\text{C}=\text{N}$ and $\text{C}=\text{O}$ groups (heterocyclic system)] resulted from the hydrolysis and oxidation of the main chains [18,26].

3.3. TG, DTG and DSC Analysis

Thermal analyses were conducted to characterize in detail the polymer and its thermal behavior. Thermal analysis was chosen since many properties of a complex sample can be obtained, as described as follows. The TG relates the behavior of a sample's weight and physicochemical phenomena. Through DTG, it is possible to gain information of the temperature and enthalpy at which thermal phenomena occur; and DSC was used to study the thermal transitions of the polymer while it is heated.

The TG thermogram of HCN-DTP is shown in Figure 2. In accordance with earlier reports about the thermogravimetric behavior of HCN-derived polymers, three stages can be identified: (I) a drying state ($<150\text{ }^\circ\text{C}$), (II) a pyrolysis stage ($150\text{--}450\text{ }^\circ\text{C}$), and (III) a carbonization stage ($>450\text{ }^\circ\text{C}$) [17,18,27,28,53].

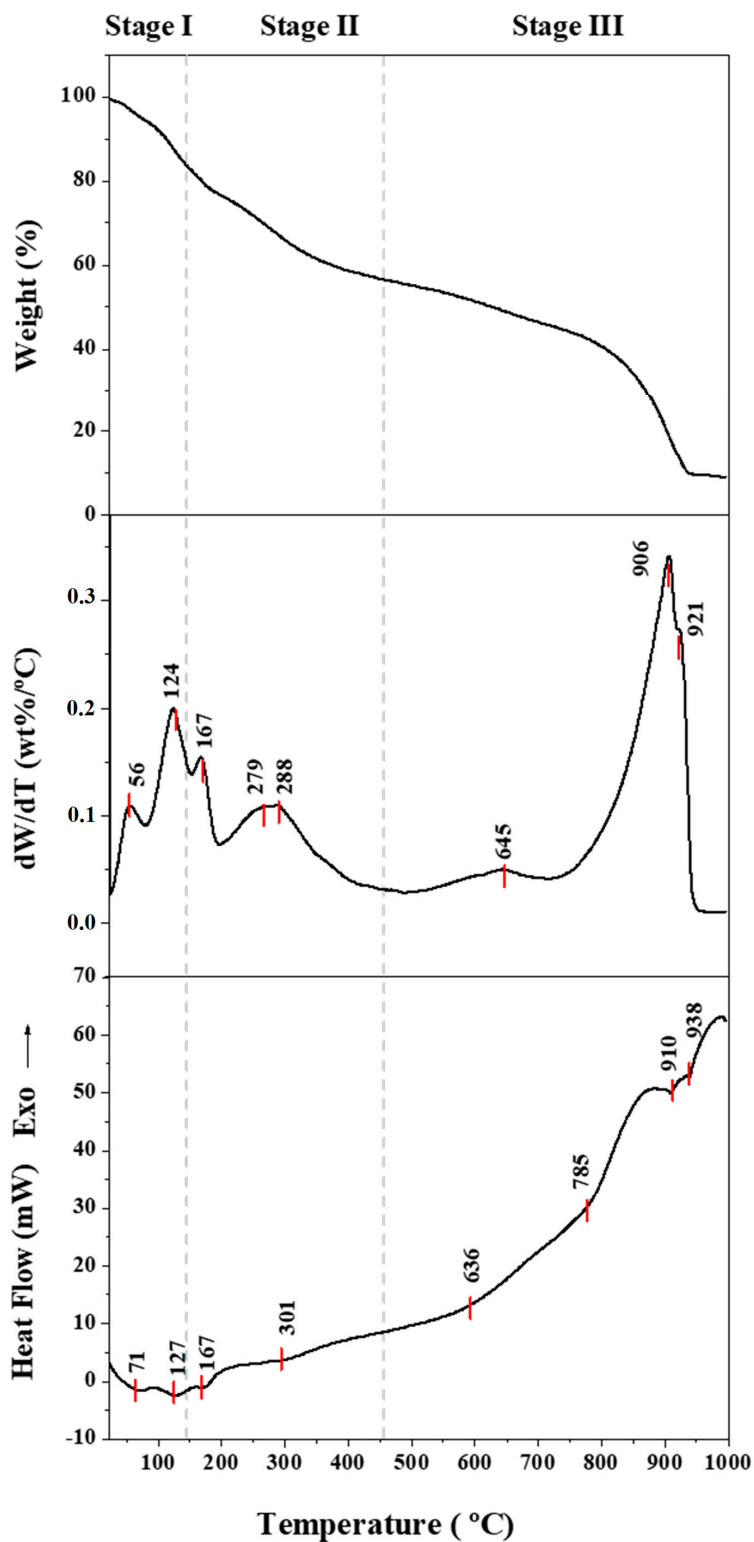


Figure 2. Thermogravimetric (TG), differential thermal analysis (DTG), and differential scanning calorimetry (DSC) curves. The predominant thermal peak around 900 °C is markedly different from previous reports. The DTG curve shows common decomposition steps related with HCN-derived polymers. However, the peak at 167 °C and the peaks around 900 °C are unique of our sample. The DSC curve shows multiple thermal decomposition steps. In general, each peak has its corresponding peak in the DTG curve.

At the first stage, there is a mass loss in our sample of about 17.2 wt %. In this stage, only one peak has been reported [18,27,28]. However, two other evident peaks (at 55 and 124 °C) can be observed in our sample, which suggests two main decomposition steps during the evaporation process. The dehydration occurs at low temperatures (<90 °C), which suggests the general degradation profiles of HCN-derived polymers [18,27,28]. The first peak (i.e., 55 °C) is related to the release of volatile compounds such as NH₃ or H₂O, which are retained in the polymer (approximately 10 wt %). The predominant peak around 124 °C could be associated with the mass loss from the structure of the polymer. Accordingly, the value of mass loss during the first stage is 7.83 wt %. This value is consistent with previous reports (HCN-derived polymer samples present an average value close to 7.8%) [18,27,28]. It should be mentioned that the systematic procedure development by Ruiz-Bermejo and co-workers [17] consists of washing the solid insoluble black polymer in order to remove the soluble part that may be retained by the polymer. As we did not have appreciable solid particles during synthesis, this step was not carried out (see above). Therefore, it should be considered that the peaks at the first stage may correspond to the soluble part retained by the polymer.

The first stage corresponds to the vaporization of moisture and the desorption of water. Likewise, it has been reported that the differences among HCN-derived polymers in this stage may be linked with the tendency to absorb atmospheric moisture (hydrophilicity) [18]. The synthesis of HCN-DTP was performed under argon atmosphere, and furthermore, the polymerization reaction was performed under depleted oxygen conditions. The higher hydrophilicity of our sample may be related with moisture directly acquired from aqueous medium resulted from hydrolysis reactions (e.g., hydrolysis of nitriles, urea, and/or diiminosuccinonitrile, DISN [32,33]). Hence, the peak at 124 °C in our sample could be linked with another thermal event, the degradation of other organic molecules, such as urea, which are ionically adsorbed on the polymer backbone.

The mass loss at the second stage (26.1%) and the last stage (46.8%) are similar to other HCN-derived polymers' behavior, corresponding to a mass loss of approximately 25 wt % and 48 wt %, respectively [18,27,28]. The second thermal degradation is associated with the thermal decomposition of the weakest bonds (e.g., side groups on the main chain); while the third stage is related with the breaking of the main chain. Previous reports [18,27,28] have suggested a correlation between the mass loss at these stages, with longer polymerization time, and furthermore, a higher thermal stability. In addition, two clear DTG peaks appear at 167 °C, and around approximately 280 °C, a well-defined peak is also found at 288 °C, and a slight shoulder is around 279 °C. Due to the proximity of these peaks, we will refer only to the peaks at 167 °C and 288 °C as part of the second stage (Figure 2). These peaks may be related with secondary scissions, which are associated with relative high stability structures [28]. Although, in general, two well-defined peaks at >200 °C are identified in this second zone, other peaks can be present depending on the HCN-derived polymer (e.g., aqueous polymerization of DAMN at 80 °C and DuPont's sample show clear peaks above 390 °C) [18,27,28]. No peaks have been reported at the second degradation stage at temperatures <200 °C. Hence, the sharp peak around 167 °C might be associated with a specific thermal decomposition step in HCN-DTP.

Significant differences, due to thermal degradation of the main chain of HCN-derived polymers, are associated with the third stage [18,27,28]. Our sample yields approximately 10 wt % of char residue at 1000 °C, which is lower than the reported values (i.e., >15 wt %) (Table S1). A slow rate of weight loss around 642 °C is consistent with the general behavior of HCN-derived polymers [18,27,28]. Moreover, two predominant peaks are found at 906 °C and 921 °C, with a rate of weight loss that is quite fast, which are the main degradation events of our sample. Char forming reaction can be associated with the last peak (approximately 921 °C) under coupled thermal events. This result suggest that the HCN-DTP is more stable than the predominant HCN-derived polymer (i.e., synthesized from cyanide salts, AMN or DAMN) [18,27,28]; this difference may be associated with the synthesis procedure. It has been suggested that the high thermal properties of HCN-derived polymers are related with the high interaction between polymer chains and rigid chain-stiffening (cross-linked structures and rigid chains with hetero/aromatic structures along the backbone); their decomposition involves the chemical conversion of side chains [28]. Likewise, the presence of an oxygen atmosphere seems to have an effect

during the last part of thermal degradation, since there is no char residue due to thermo-oxidation processes [27,28].

As our polymer was synthesized under free oxygen atmosphere, the greatest peaks around 900 °C may be related with a char-forming reaction that is a result of important cross-linking reaction associated with oxygen atoms inside the polymer structure. Only one study reported a relevant degradation step around 900 °C [28]. This high thermal stability can be associated with a higher oxygen content in the HCN polymers, which depends on polymerization reactions or on the oxygenated functional groups in the macromolecular structure due to hydrolytic processes. Some plausible structures have been reported for oxidized HCN-derived polymers which are enriched in keto groups, amino acids, hydroxy acids, primary amides, and carboxylic acids; these structures are the result of hydrolysis reaction from imine, amino nitriles, cyanohydrins, cyano, and amide groups, respectively [28].

Although the thermal behavior of HCN-derived thermal polymer is complex, characteristic peaks are summarized in Table 1. In general, we can associate each peak with endothermic (DSC) degradation processes. The analysis of the DTG curves shows at least seven predominant peaks associated with different thermal events. These peaks are numbered according to gradual appearance, as a function of temperature.

Table 1. Characteristic temperatures for the thermal decomposition of HCN-thermal derived polymer under argon atmosphere. DTG maxima with the corresponding rates of weight loss, dW/dt, and DSC peaks observed in the samples.

Peak	Stage I (25–150 °C) Evaporation			Stage II (150–450 °C) Low Thermal Decomposition			Stage III (450–1000 °C) High Thermal Decomposition				
	DTG	DSC	Peak	DTG	DSC	Peak	DTG	DSC			
	T _{max} (°C)	dW/dt (wt %/°C)	T _{peak} (°C)	T _{max} (°C)	dW/dt (wt %/°C)	T _{peak} (°C)	T _{max} (°C)	dW/dt (wt %/°C)	T _{peak} (°C)		
1	56	0.11	71	3	167	0.15	167	5	636	0.05	636
2	124	0.20	127	4	279	0.11					785
					288	0.11	301	6	906	0.34	910
								7	921	0.27	938

The DSC thermogram is shown in Figure 2 along with its corresponding peak temperatures (T_{peak}) (Table 1). The different peaks can be attributed to several decomposition/oxidation reactions associated with deamination, dehydration, and decyanation as the main reactions. At higher temperatures, random breaking by heteroatom bridges can occur [28]. Finally, carbonaceous char could result from cyclization (exothermic events associated with the heating of nitrile polymers), scission, and cross-linking reactions. The cyclization may occur during HCN polymerization, through nitrile groups forming a stable ladder backbone [17,27,28]. Two endothermic peaks are clearly observed around 900 °C.

In summary, the high oxidation degree of the structure of the HCN-DTP could result from a continuous hydrolysis, deamination, and decyanogenation process, along polymerization. These reactions generate a complex macromolecular structure that is essentially a polyamide with intra and inter amide bonds, as suggested recently [28].

3.4. Mass Spectrometric Thermal Analysis

The functional groups of the decomposition residues were determined by in situ mass spectrometry (MS). It was possible to detect several volatile species from the thermal decomposition and fragmentation processes of the HCN-DTP polymer (Figure 3). As in the thermogravimetric analysis, we considered the same three thermal decomposition stages to compare its analysis with DTG and DSC curves. Several signals have been observed for MS peaks in a wide range of temperatures. Major signals have been quite well characterized, and they are associated with H₂O, NH₄⁺ (*m/z* = 18), and OH⁻ and NH₃ (*m/z* = 17, Figure 3a) [27,28,53]. Clear MS peaks at 61, 122, and 293 °C are observed for the H₂O/NH₄⁺ profile. A broad peak, from 700 up to 850 °C, is present. Two evident signals at 61 °C and

markedly at 172 °C related with other amine species (i.e., $m/z = 15$, NH, $m/z = 16$, NH₂ and $m/z = 17$, NH₃/OH⁻) and NO ($m/z = 30$) are observed. Two broad peaks can be recognized among 200–600 °C for NH and NO (Figure 3a), and it may contribute to the predominant signal on the second stage (279–288 °C) (Table 1). These profiles (Figure 3a) coincide with the first four mass loss observed on DTG curves (Figure 2) and are associated with deamination process, and the releasing of physisorbed water. Besides the mentioned products, other obvious MS peaks are present with a considerable intensity. Probably, carbon and/or nitrogen species (e.g., C⁺ ($m/z = 12$); N/CH₂⁺ ($m/z = 14$); CO/N₂ ($m/z = 28$); HCO ($m/z = 29$) and CO₂/HC(=NH)NH₂ ($m/z = 44$); Figure 3b) contribute to the mass loss at the first stage (approximately 122 °C) and along a broad temperature interval on the second stage (172 and 250–303 °C). For example, the profiles of $m/z = 12$ (e.g., C) and $m/z = 44$ (e.g., CO₂/HC(=NH)NH₂) show similar behavior. A first peak appears around 122 °C, two signals appear at the second stages (i.e., 172 and 253–273 °C), and three clear signals appear at the third stage (i.e., for CO₂; 643, 793, and 903 °C). In general, these temperature profiles display similar MS peaks to those ion currents corresponding to scission and/or depolymerization mechanisms (i.e., deamination, denitrogenation, decarboxylation, and decyanogenation) [27,28,53]. The signal at $m/z = 44$ also can be attributed to the hydrolytic cleavage of the amide linkage, which can lead to the formation of two fragments with NH₂ and COOH end groups.

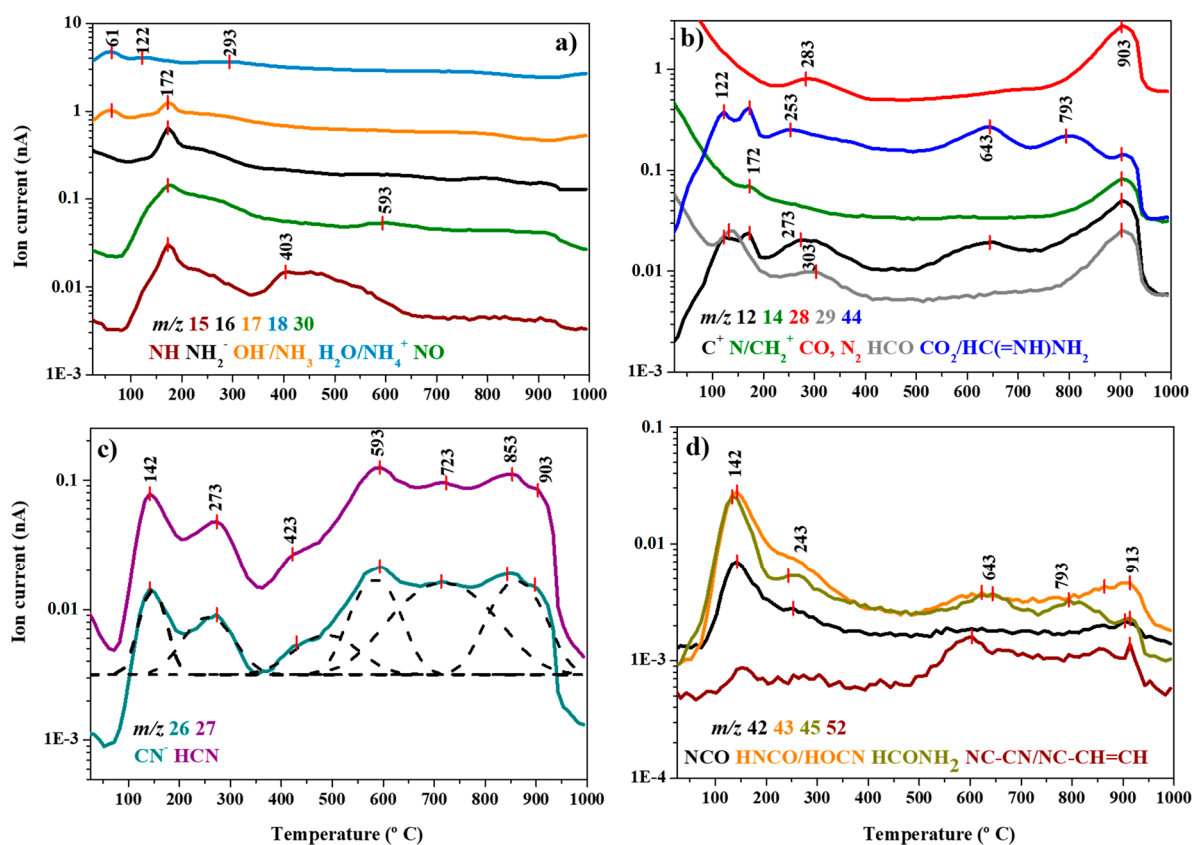


Figure 3. Ion intensity curves for HCN-derived thermal polymer. Deamination and decarboxylation mechanisms during pyrolysis stages dominate over dehydration. (a) Major signals associated with the releasing of amines and water; (b) signals associated with carbon and nitrogen species released through scission and/or depolymerization mechanisms; (c) cyanide and HCN curves; and (d) signals associated with the cleavage of the polymer chain through the release of larger species.

As was mentioned before, the most intense peak on the DTG curve is around 900 °C. The profiles of carbon/nitrogen species show a well-defined and intense peak around 903 °C (Figure 3b); this peak is the

result of diverse species that could include C^+ , CH_2^+ , CO , HCO , $CO_2/HC(=NH)NH_2$ through cracking of the HCN polymer main chain, such as $-N=N-$ or $-HC=O$ or $-N=C=O$ and/or by decarboxylation.

Cyanide and hydrogen cyanide curves for $m/z = 26$ and $m/z = 27$, respectively, are shown in Figure 3c. In order to examine carefully these profiles, an analysis based on a Gaussian function for the deconvolution method was performed. The deconvolution analysis shows at least six peaks that resemble very well the last six predominant peaks on the DTG profile (Figure 2). It must be considered that although the profile resembles the general decomposition process, the intensity of the signals associated to cyanide species are less intense (approximately 10 times) than the signals associated with the decarboxylation process (Figure 3b). However, it is possible to deduce that decyanogenation of the polymer takes place over a wide range of temperatures (from 142 up to 903 °C).

Finally, the TG-MS profiles for $m/z > 30$ (Figure 3d) produce clear signals along the first two thermal stages (i.e., 142 and 243 °C) that may be the result of the cleavage of the polymer chain through the release of NCO ($m/z = 42$), isocyanic acid, and/or cyanic acid ($m/z = 43$), the corresponding deprotonated derivate of formamidine ($^+C(=NH)NH_2$ $m/z = 43$), formamide ($m/z = 45$), and $NC-CH=CH^-$ ($m/z = 52$). Other appreciable peaks are characteristic for the third stage (i.e., 643, 793, and 913 °C). The fragment at $m/z = 52$ can be attributed to dinitrile $NC-CN$ or mononitrile derivative (the fragment $NC-CH=CH^-$) from polyaminonitrile, as it has been suggested in previous reports [27,28,53]. No more important signals were detected for $m/z > 52$.

In general, the TG-MS profiles and DTG curves are consistent with the thermal behavior of HCN-DTP. Table 2 shows a simpler view of the contribution of each volatile species related with different thermal stages.

Table 2. Summary of detected feasible volatile species associated with each stage of thermal decomposition and fragmentation processes of HCN-derived thermal polymer (HCN-DTP).

Probable Species	MS Peaks (m/z)	DTG Peaks (°C)						
		55	124	167	279–288	642	906	921
C^+	12							
N, CH_2^+	14							
NH	15							
NH_2	16							
OH^-, NH_3	17							
H_2O/NH_4^+	18							
^-CN	26							
HCN	27							
CO, N_2	28							
N_2H, HCO	29							
NO	30							
NCO	42							
HNCO, HOCN	43							
CO_2	44							
$^+C(=NH)NH$	45							
$HCONH_2$	45							
$NC-CN,$	52							
$NC-CH=CH$	52							
STAGES		STAGE I		STAGE II		STAGE III		

Note: Except for, water, ammonia, and nitrile oxides, all species contribute with the greatest thermal step showed on the DTG curve.

In summary, it is possible to distinguish among species with punctual thermal events from those that decomposed gradually. The first stage (<150 °C) seems to be associated with the release of physisorbed water, deamination, and the cleavage of the polymer chain through the release of high mass species. The second and the last stages are the result of continuous decyanogenation, deamination, and decarboxylation mechanisms. The almost identical behavior between the carbon profile and carbon dioxide suggests that decarboxylation is the main thermal decomposition process, which is consistent with a high oxygenated structure of the polymer.

The HCN-DTP polymer is extremely complex, and many of its functional groups were determined by in situ mass spectrometry. The potential of this polymer as a source for organic molecules motivated

conducting hydrolysis experiments in order to identify released organics that are relevant for prebiotic chemistry studies.

3.5. GC-MS Analysis of Hydrolyzed Samples

Acidic and basic hydrolyses were performed in order to release organics from the synthesized polymer. In our case, a series of polar organic compounds, after acidic hydrolysis treatment, were identified (Figure 4). The basic treatment only released a very small fraction of organic compounds (i.e., glycolic acid, aminomalonic acid, and urea) (figure not shown).

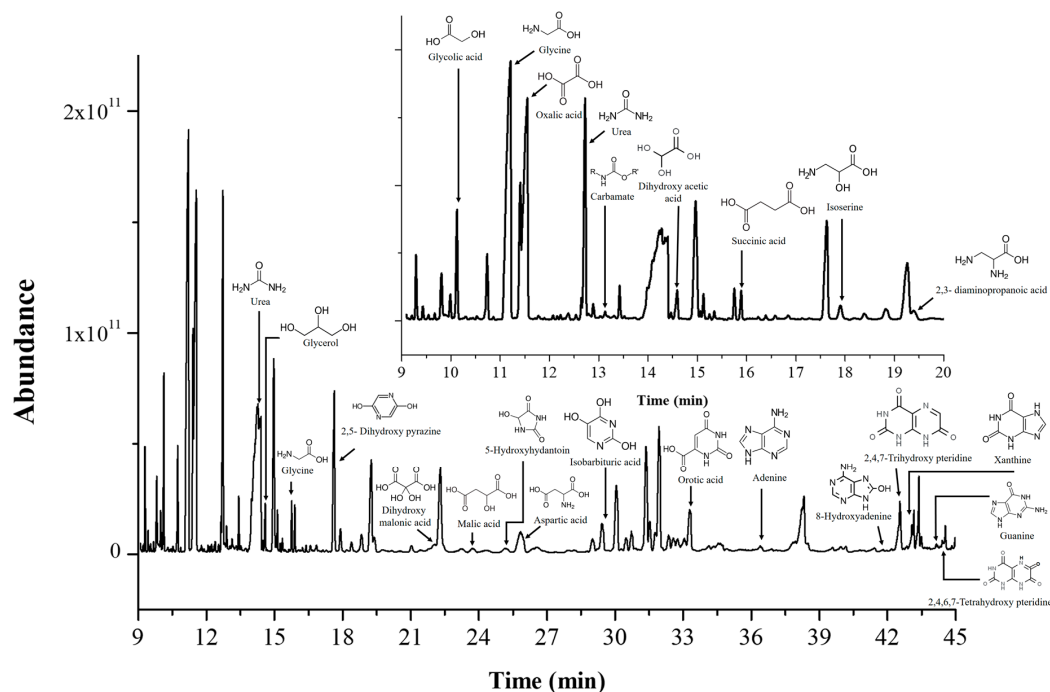


Figure 4. GC-MS chromatogram of hydrolyzed HCN-DTP samples. The profile shows some organic molecules released after acid hydrolysis.

Around 100 different organic compounds have been characterized after the hydrolysis of HCN-derived polymers [2,17,19–21,61,63,64]. Synthesis and hydrolysis conditions (i.e., differences in heating time and pH value) determine the amount and the chemical species released [19,60,65,66]. For example, the hydrolysis of aminomaleonitrile polymer, AMN polymer, showed that basic hydrolysis yields higher amounts of α -amino acids than acidic hydrolysis [67]. The acidic hydrolysis release more organic molecules than basic treatment [19]. In our case, in both hydrolysis treatments, urea was the most representative species. Moreover, after acidic treatment, the detected species are predominantly N-heterocyclic compounds (e.g., purines such as adenine, guanine, 8-hydroxyadenine, and xanthine; pyrimidines such as isobarbituric acid and orotic acid; pteridines such as 2,4,7-trihydroxypteridine and 2,4,6,7-tetrahydroxypteridine; and 2,5-dihydroxy pyrazine and 5-hydroxy hydantoin) carboxylic acids (e.g., glycolic acid, oxalic acid, 2-dihydroxy acetic acid, succinic acid, dihydroxymalonic acid, and malic acid) and amino acids (e.g., glycine, 2,3-diaminopropanoic acid, aspartic acid, and isoleucine). Hence, the restrictive variability of chemical species from HCN-DTP could be associated to its synthesis.

An interesting analysis of the insoluble residues after acid hydrolysis of NH_4CN -derived polymers showed that high temperatures are correlated with the stability of the macromolecular structure [26]. In other words, the polymers formed at high temperatures are more stable against acid hydrolysis. In this way, we can hypothesize two probable scenarios. On the one hand, the high stability of HCN-DTP (see above) does not lead to the easy release of simpler organic compounds. On the other hand, as it has been suggested before [17], the formation of a non-hydrolyzable matrix (heterocyclic

macrostructure) results in the releasing of organic molecules that were retained within the structure; this retention is lower at high temperatures. Since the high temperatures yields high stable macrostructures, the retention of organic molecules is not efficient (non-available retention spaces) and in consequence, the amount and diversity of molecules is limited. In addition, as the basic treatment was performed at a lower heating time, the pool of organic compounds is limited.

In summary, the systematic method followed in this report suggests that HCN-DTP can be understood as a highly oxidized macrostructure with conjugated carbon and nitrogen bonds. As it has been reported recently, the physicochemical properties of these materials are directly related with temperature and raw material, which favors hydrolytic and/or oxidative reactions during the polymerization of HCN [18,26]. The identification of the physicochemical properties of this polymer is crucial to propose a scenario where the HCN-DTP could have played an important role from the point of view of chemical evolution.

4. Discussion

Since the 1970s, it has been proposed that hydrogen cyanide can play an important role in the formation of complex organic molecules under hydrothermal conditions [5,40–46]. In addition, new ideas propose the surroundings of alkaline environments as ideal niches for a rich HCN chemistry [9,68,69]. If HCN was present in alkaline hydrothermal environments, as suggested by Holm and Neubeck [5], the reactions it will undergo would be crucial to understand its role in prebiotic reactions occurring on these environments. Figure 5 shows a possible scenario of the probable fate of HCN, as well as its thermal polymer, under a submarine alkaline hydrothermal system.

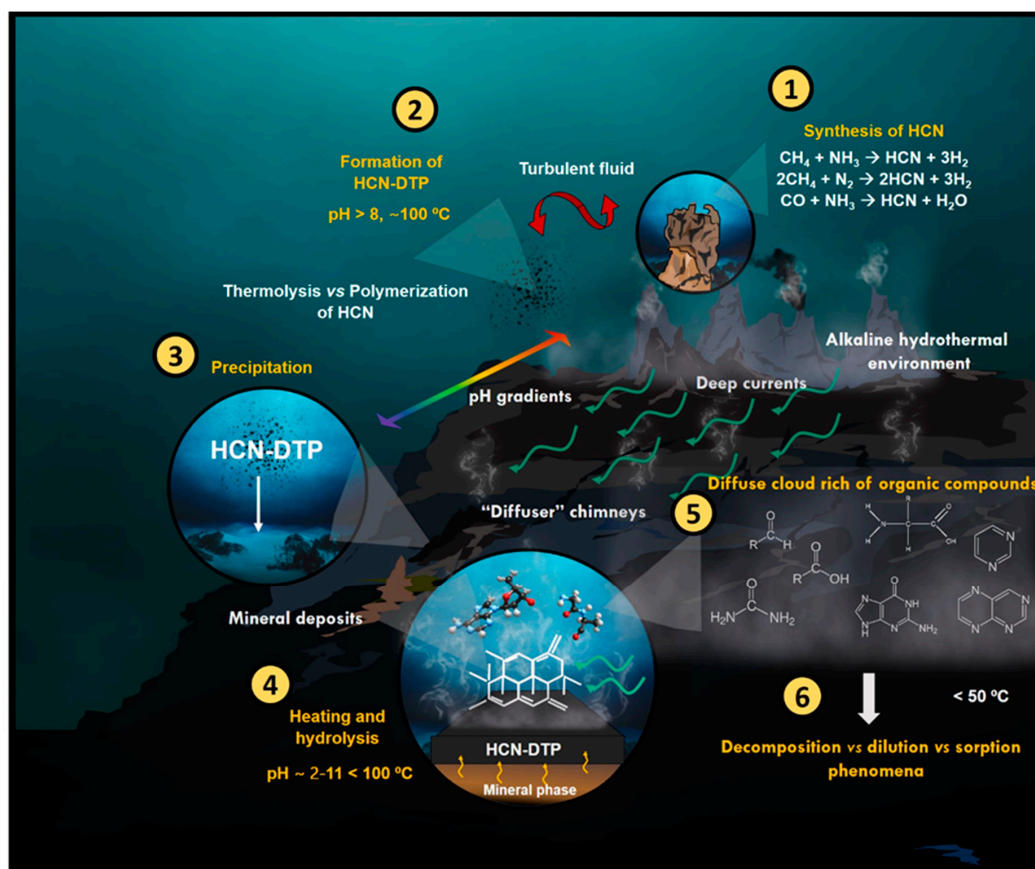


Figure 5. Probable fate of HCN and its thermal polymer (HCN-DTP) in a primitive submarine hydrothermal system. Each point is described in detail in the text.

The availability of HCN in submarine hydrothermal systems similar to the Lost City in the Hadean Earth [5,70,71] allow HCN through two main reaction pathways. As soon as the HCN is synthesized (from the released gases, e.g., CH₄, NH₃, CO, N₂) in hydrothermal fluids (Figure 5, Step 1), a continuous competition among hydrolysis [68] and polymerization reactions takes place [26,54]. In a recent paper [52], we showed that the thermolysis of HCN at relatively alkaline pH values (i.e., pH > 8) allows the formation of a kind of HCN-DTP.

Higher pH values (i.e., pH > 10) may favor the formation of the HCN-DTP polymer (Figure 5, Step 2) over HCN hydrolysis at relatively high temperatures (this work). Once HCN-DTP is formed, it will experience several phenomena; the turbulent fluids and the deep currents could spread it along the hydrothermal system. As it is essentially insoluble, eventually, it will precipitate (Figure 5, Step 3) at lower temperatures (<100 °C) and may interact with mineral surfaces.

In hydrothermal systems, there are both temperature and pH gradients naturally occurring (Figure 5, Step 4). The HCN polymer could be exposed to a wide temperature gradient (from 2 up to 350 °C), and along with pH variations, hydrolysis could accomplish. Hydrothermal deposits and venting sites along hydrothermal systems with temperatures below 100 °C represent big areas (spanning a few kilometers) [72–75]. In addition, the dynamic flux could generate important pH gradients through the circulation of fluids [76]. In this way, the polymer could be heated at temperatures as high as 300 °C at different pH values. Although the off-axis (e.g., the Lost City Hydrothermal System) ultramafic hosted hydrothermal systems are essentially alkaline environments, the contribution of acid fluids from relative near ultramafic on-axis systems (e.g., the Rainbow Hydrothermal System) [77] could favor acidic hydrolysis (pH < 3). As the thermal behavior suggests (see above), the heating (<300 °C) of HCN polymers would release several organic species to the environment. In particular, the acid hydrolysis coupled with heating would favor the release of organic compounds of prebiotic interest (e.g., aldehydes, carboxylic acids, amino acids, and N-heterocyclic compounds). These results are consistent with previous works that highlight the relevance of submarine alkaline hydrothermal systems. For example, La Rowe and Regnier [71], based on theoretical analysis, showed that under hydrothermal conditions (i.e., off-axis vent sites, 150 °C, 500 bars), HCN reacts with dissolved gases (e.g., CO₂, H₂, N₂), forming nucleobases through the formation of HCN polymer. A cloud rich of organic compounds could be formed surrounding hydrothermal systems (Figure 5, Step 5). The organic molecules could have persisted at high temperatures and pressures since, as it has been discussed, the fate of organic molecules depends on the particular environmental conditions [50,58]. For instance, it has been proven that some amino acids (e.g., lysine and glutamic acid) are thermally more stable under alkaline solutions at high temperatures (>200 °C) [78].

The species (organics, gases, ions, metals, and minerals) in hydrothermal systems could be transported [79] to other primitive environments, where they could follow decomposition, dilution, precipitation, and/or sorption processes [80] (Figure 5, Step 6). In this experiment, the release of adenine from HCN polymer was confirmed. The availability of N-heterocyclic compounds is crucial to the formation of RNA oligomers. It has been suggested that RNA polymerization could probably occur at conditions similar to those found on submarine hydrothermal systems [81]. The formation of other complex molecules, tholins, has been studied under alkaline conditions [82]. In this study, the formation of alkaline aqueous aerosols under reducing atmospheres (e.g., NH₃, CH₄, H₂) resulted in a great diversity of organic molecules, notably glyoxylic acid, which has a great relevance in the hypothesis of glyoxylate. This finding highlights that the synthesis of organics could be favored by alkaline conditions.

This research is part of a series of prebiotic chemistry experiments devoted to understanding the behavior of a very simple molecule (HCN) exposed to conditions found on Hydrothermal Vents Systems. In this research, the main objective was to characterize the produced polymer and to identify the released formed products. In the field of prebiotic chemistry, we try to find conditions that allowed the increase in the complexity of molecules through the simulation of feasible environments and including some likely variables in them. The formation of more complex molecules than those we

used as raw material could have led to the development of interactions among these molecules and thus accomplish a complex chemistry. Eventually, such scenarios could have preceded the origin of life on Earth.

5. Conclusions

HCN is abundant throughout the universe, and it can be easily formed in hydrothermal chimneys. In this work, we explored the synthesis and characterization of an HCN polymer produced under conditions resembling those of HV. Our results support the hypothesis developed by Nils Holm and co-workers about the relevance of alkaline systems to host a rich chemistry during the first steps of chemical evolution [5,83]. The synthesis of HCN-DTP polymer under assayed conditions, simulating alkaline hydrothermal conditions, reinforce the idea about considering those environments as relevant during early Earth for organic synthesis. HCN polymers are a huge group of macromolecules, and their study requires the use of different analytical techniques. The polymer synthesized in this experiment is very complex and presents chemical properties different from those of the already characterized polymers. After hydrolysis, it releases prebiotic relevant molecules such as purines, pyrimidines, carboxylic acids, and amino acids.

The next step in this study could be to focus on understanding the effect of ions and mineral surfaces in the synthesis of those polymers and to evaluate their effects on the production of complex organic molecules. In addition, as pressure is a key variable in submarine hydrothermal systems (since it affects the boiling point of water, and a change in pressure could affect the polymer yield and the selectivity of the reaction), in a future work, we aim to develop this idea.

Although this research focuses on studying the role of HCN-DTP in alkaline hydrothermal systems and its impact on chemical evolution, the conditions for its synthesis are easily applied to materials science. Likewise, characterizing its physicochemical properties may be useful for other approaches and expand to other research areas.

Supplementary Materials: The following are available online at <http://www.mdpi.com/2227-9717/8/8/968/s1>. Table S1: Summary of HCN-derived polymers from diverse synthesis, Table S2: Description and assignation of IR bands for HCN-DTP.

Author Contributions: Conceptualization, M.R.-B. and M.C.-G.; methodology M.R.-B.; validation, S.A.V.-B., P.R.-P., and M.R.-B.; formal analysis, S.A.V.-B. and P.R.-P.; investigation, S.A.V.-B.; resources, M.R.-B.; writing—original draft preparation, S.A.V.-B., M.C.-G. writing—review and editing, M.C.-G.; supervision, M.R.-B. and M.C.-G.; funding acquisition, M.R.-B. and M.C.-G. All authors have read and agreed to the published version of the manuscript.

Funding: This research was funded by the project ESP2017-89053-C2-2-P from the Spanish Ministerio de Ciencia, Innovación y Universidades; the project MDM-2017-0737 Centro de Astrobiología (CSIC-INTA), Unidad de Excelencia María de Maeztu from the Spanish State Research Agency (AEI), the DGAPA-PAPIIT (grant number IA203217), and CONACyT (grant A1-S-25341).

Acknowledgments: S.A.V.-B. acknowledges Posgrado en Ciencias de la Tierra UNAM, CONACyT (Ph. D. grant 697442 and the financial support for a research stay grant) and the technical assistance of Claudia Camargo. The Instituto de Ciencias Nucleares (UNAM), and Centro de Astrobiología (CAB) are acknowledged for the use of their facilities. M.R.-B. and P.R.-P. used the research facilities of the Centro de Astrobiología (CAB) and were supported by the Instituto Nacional de Técnica Aeroespacial “Esteban Terradas” (INTA) and by the Spanish State Research Agency (AEI) Centro de Astrobiología (CSIC-INTA), Unidad de Excelencia María de Maeztu. Additionally, the authors are grateful to M^a Teresa Fernández for performing the FT-IR spectra, and to the “Servicio de Análisis Térmico” of ICMN (CSIC, Spain).

Conflicts of Interest: The authors declare no conflict of interest. The funders had no role in the design of the study; in the collection, analyses, or interpretation of data; in the writing of the manuscript, or in the decision to publish the results.

References

1. Sutherland, J.D. The Origin of Life—Out of the Blue. *Angew. Chem. Int. Ed.* **2016**, *55*, 104–121. [[CrossRef](#)] [[PubMed](#)]

2. Ruiz-Bermejo, M.; Zorzano, M.P.; Osuna-Esteban, S. Simple Organics and Biomonomers Identified in HCN Polymers: An Overview. *Life* **2013**, *3*, 421–448. [[CrossRef](#)] [[PubMed](#)]
3. Ferris, J.P.; Hagan, W.J. HCN and chemical evolution: The possible role of cyano compounds in prebiotic synthesis. *Tetrahedron* **1984**, *40*, 1093–1120. [[CrossRef](#)]
4. Matthews, C.N.; Minard, R.D. Hydrogen cyanide polymers, comets and the origin of life. *Faraday Discuss.* **2006**, *133*, 393–401. [[CrossRef](#)]
5. Holm, N.G.; Neubeck, A. Reduction of nitrogen compounds in oceanic basement and its implications for HCN formation and abiotic organic synthesis. *Geochem. Trans.* **2009**, *10*, 9. [[CrossRef](#)]
6. Tian, F.; Kasting, J.F.; Zahnle, K. Revisiting HCN formation in Earth's early atmosphere. *Earth Planet. Sci. Lett.* **2011**, *308*, 417–423. [[CrossRef](#)]
7. Parkos, D.; Pikus, A.; Alexeenko, A.; Melosh, H.J. HCN production from impact ejecta on the early Earth. In Proceedings of the 30th International Symposium on Rarefied Gas Dynamics: RGD 30, Victoria, BC, Canada, 10–15 July 2016; AIP Publishing: Melville, NY, USA; Volume 1786, p. 170001.
8. Ferus, M.; Kubelík, P.; Knížek, A.; Pastorek, A.; Sutherland, J.; Civiš, S. High energy radical chemistry formation of HCN-rich atmospheres on early Earth. *Sci. Rep.* **2017**, *7*, 6275. [[CrossRef](#)]
9. Rimmer, P.B.; Shorttle, O. Origin of life's building blocks in carbon-and nitrogen-rich surface hydrothermal vents. *Life* **2019**, *9*, 12. [[CrossRef](#)]
10. Colín-García, M.; Negrón-Mendoza, A.; Ramos-Bernal, S. Organics produced by irradiation of frozen and liquid HCN solutions: Implications for Chemical Evolution Studies. *Astrobiology* **2009**, *9*, 279–288. [[CrossRef](#)]
11. Mumma, M.J.; Charnley, S.B. The chemical composition of comets—Emerging taxonomies and natal heritage. *Annu. Rev. Astron. Astrophys.* **2011**, *49*, 471–524. [[CrossRef](#)]
12. Pizzarello, S. Hydrogen cyanide in the Murchison meteorite. *Astrophys. J. Lett.* **2012**, *754*, L27. [[CrossRef](#)]
13. Stribling, R.; Miller, S.L. Energy yields for hydrogen cyanide and formaldehyde syntheses: The hcn and amino acid concentrations in the primitive ocean. *Orig. Life Evol. Biosph.* **1987**, *17*, 261–273. [[CrossRef](#)] [[PubMed](#)]
14. Miyakawa, S.; Cleaves, H.J.; Miller, S.L. The cold origin of life: A. Implications based on the hydrolytic stabilities of hydrogen cyanide and formamide. The cold origin of life: A. Implications based on the hydrolytic stabilities of hydrogen cyanide and formamide. *Orig. Life Evol. Biosph.* **2002**, *32*, 195–208. [[CrossRef](#)] [[PubMed](#)]
15. Fábíán, B.; Szőri, M.; Jedlovszky, P. Floating Patches of HCN at the Surface of their aqueous solutions—Can they make “HCN World” Plausible? *J. Phys. Chem. C* **2014**, *118*, 21469–21482. [[CrossRef](#)]
16. Liebman, S.A.; Pesce-Rodriguez, R.A.; Matthews, C.N. Organic analysis of hydrogen cyanide polymers: Prebiotic and extraterrestrial chemistry. *Adv. Space Res.* **1995**, *15*, 71–80. [[CrossRef](#)]
17. Ruiz-Bermejo, M.; de la Fuente, J.L.; Rogero, C.; Menor-Salván, C.; Osuna-Esteban, S.; Martín-Gago, J.A. New insights into the characterization of ‘insoluble black HCN polymers. *Chem. Biodivers.* **2012**, *9*, 25–40. [[CrossRef](#)] [[PubMed](#)]
18. Ruiz-Bermejo, M.; José, L.; Carretero-González, J.; García-Fernández, L.; Aguilar, M.R. A Comparative Study on HCN Polymers Synthesized by Polymerization of NH₄CN or Diaminomaleonitrile in Aqueous Media: New Perspectives for Prebiotic Chemistry and Materials Science. *Chem. Eur. J.* **2019**, *25*, 11437–11455. [[CrossRef](#)]
19. Ferris, J.P.; Wos, J.D.; Nooner, D.W.; Oró, J. Chemical evolution: XXI. The Amino Acids Released on Hydrolysis of HCN Oligomers. *J. Mol. Evol.* **1974**, *3*, 225–231. [[CrossRef](#)]
20. Matthews, C.N.; Moser, R.E. Peptide synthesis from hydrogen cyanide and water. *Nature* **1967**, *215*, 1230–1234. [[CrossRef](#)]
21. Oró, J.; Kimball, A.P. Synthesis of purines under possible primitive earth conditions. I. Adenine from hydrogen cyanide. *Arch. Biochem. Biophys.* **1961**, *94*, 217–227. [[CrossRef](#)]
22. Thissen, H.; Koegler, A.; Salwiczek, M.; Easton, C.D.; Qu, Y.; Lithgow, T.; Evans, R.A. Prebiotic-chemistry inspired polymer coatings for biomedical and material science applications. *NPG Asia Mater.* **2015**, *7*, e225. [[CrossRef](#)]
23. Thissen, H.; Evans, R.; Koegler, A. Hydrogen Cyanide-Based Polymer Surface Coatings and Hydrogels. U.S. Patent 9,587,141, 17 May 2017.
24. Toh, R.J.; Evans, R.; Thissen, H.; Voelcker, N.H.; d'Ischia, M.; Ball, V. Deposition of Aminomalononitrile-Based Films: Kinetics, Chemistry, and Morphology. *Langmuir* **2019**, *35*, 9896–9903. [[CrossRef](#)] [[PubMed](#)]

25. D'Ischia, M.; Manini, P.; Moracci, M.; Saladino, R.; Ball, V.; Thissen, H.; Evans, R.A.; Puzzarini, C.; Barone, V. Astrochemistry and Astrobiology: Materials Science in Wonderland? *Int. J. Mol. Sci.* **2019**, *20*, 4079.
26. Mas, I.; de la Fuente, J.L.; Ruiz-Bermejo, M. Temperature effect on aqueous NH₄CN polymerization: Relationship between kinetic behaviour and structural properties. *Eur. Polym. J.* **2020**, *132*, 109719. [[CrossRef](#)]
27. José, L.; Ruiz-Bermejo, M.; Nna-Mvondo, D.; Minard, R.D. Further progress into the thermal characterization of HCN polymers. *Polym. Degrad. Stab.* **2014**, *110*, 241–251.
28. Ruiz-Bermejo, M.; de la Fuente, J.L.; Marín-Yaseli, M.R. The influence of reaction conditions in aqueous HCN polymerization on the polymer thermal degradation properties. *J. Anal. Appl. Pyrolysis* **2017**, *124*, 103–112.
29. Cataldo, F.; Patanè, G.; Compagnini, G. Synthesis of HCN polymer from thermal decomposition of formamide. *J. Macromol. Sci. A Pure Appl. Chem.* **2009**, *46*, 1039–1048. [[CrossRef](#)]
30. Cataldo, F.; Lilla, E.; Ursini, O.; Angelini, G. TGA–FT-IR study of pyrolysis of poly (hydrogen cyanide) synthesized from thermal decomposition of formamide. Implications in cometary emissions. *J. Anal. Appl. Pyrol.* **2010**, *87*, 34–44. [[CrossRef](#)]
31. Sanchez, R.A.; Ferris, J.P.; Orgel, L.E. Studies in prebiotic synthesis. II. Synthesis of purine precursors and amino acids from aqueous hydrogen cyanide. *J. Mol. Biol.* **1967**, *30*, 223–253.
32. Ferris, J.P.; Ryan, T.J. Chemical evolution. XIV. Oxidation of diaminomaleonitrile and its possible role in hydrogen cyanide oligomerization. *J. Org. Chem.* **1973**, *38*, 3302–3307. [[CrossRef](#)]
33. Ferris, J.P.; Edelson, E.H. Chemical evolution. 31. Mechanism of the condensation of cyanide to hydrogen cyanide oligomers. *J. Org. Chem.* **1978**, *43*, 3989–3995. [[CrossRef](#)]
34. Ferris, J.P.; Donner, D.B.; Lotz, W. Chemical evolution. IX. Mechanism of the oligomerization of hydrogen cyanide and its possible role in the origins of life. *J. Am. Chem. Soc.* **1972**, *94*, 6968–6974. [[CrossRef](#)]
35. Völker, T. Polymere blausäure. *Angew. Chem.* **1960**, *72*, 379–384.
36. Ferris, J.P.; Edelson, E.H.; Auyeung, J.M.; Joshi, P.C. Structural studies on HCN oligomers. *J. Mol. Evol.* **1981**, *17*, 69–77.
37. Umemoto, K.; Takahashi, M.; Yokota, K. Studies on the structure of HCN oligomers. *Orig. Life Evol. Biosph.* **1987**, *17*, 283–293.
38. Mamajanov, I.; Herzfeld, J. HCN polymers characterized by solid state NMR: Chains and sheets formed in the neat liquid. *J. Chem. Phys.* **2009**, *130*, 134503.
39. Mamajanov, I.; Herzfeld, J. HCN polymers characterized by SSNMR: Solid state reaction of crystalline tetramer (diaminomaleonitrile). *J. Chem. Phys.* **2009**, *130*, 134504.
40. Mukhin, L.E.V. Evolution of organic compounds in volcanic regions. *Nature* **1974**, *251*, 50–51. [[CrossRef](#)]
41. Mukhin, L. Volcanic processes and synthesis of simple organic compounds on primitive earth. *Orig. Life Evol. Biosph.* **1976**, *7*, 355–368. [[CrossRef](#)]
42. Dowler, M.J.; Ingmanson, D.E. Thiocyanate in Red Sea brine and its implications. *Nature* **1979**, *279*, 51–52. [[CrossRef](#)]
43. Corliss, J.B.; Baross, J.A.; Hoffman, S.E. An hypothesis concerning the relationships between submarine hot springs and the origin of life on earth. *Oceanol. Acta Spec. Issue* **1981**, *1*, 59–69.
44. Baross, J.A.; Hoffman, S.E. Submarine hydrothermal vents and associated gradient environments as sites for the origin and evolution of life. *Orig. Life Evol. Biosph.* **1985**, *15*, 327–345. [[CrossRef](#)]
45. Ferris, J.P. Chemical Markers of Prebiotic Chemistry in Hydrothermal Systems. In *Marine Hydrothermal Systems and the Origin of Life*; Holm, N.G., Ed.; Springer: Dordrecht, The Netherlands, 1992; pp. 109–134.
46. Aubrey, A.D.; Cleaves, H.J.; Bada, J.L. The Role of Submarine Hydrothermal Systems in the Synthesis of Amino Acids. *Orig. Life Evol. Biosph.* **2009**, *39*, 91–108. [[CrossRef](#)]
47. Lowe, C.U.; Rees, M.W.; Markham, R. Synthesis of Complex Organic Compounds from Simple Precursors: Formation of Amino-Acids, Amino-Acid Polymers, Fatty Acids and Purines from Ammonium Cyanide. *Nature* **1963**, *199*, 219–222. [[CrossRef](#)]
48. Hennes, R.-C.; Holm, N.; Engel, M. Abiotic synthesis of amino acids under hydrothermal conditions and the origin of life: A perpetual phenomenon? *Naturwissenschaften* **1992**, *79*, 361–365. [[CrossRef](#)]
49. Islam, M.N.; Kaneko, T.; Kobayashi, K. Determination of amino acids formed in a supercritical water flow reactor simulating submarine hydrothermal systems. *Jpn. Soc. Anal. Chem.* **2002**, *17*, i1631–i1634.
50. Colín-García, M.; Heredia, A.; Cordero, G.; Camprubí, A.; Negrón-Mendoza, A.; Ortega-Gutiérrez, F.; Beraldi, H.; Ramos-Bernal, S. Hydrothermal vents and prebiotic chemistry: A review. *Bol. Soc. Geol. Mex.* **2016**, *68*, 599–620. [[CrossRef](#)]

51. Sojo, V.; Herschy, B.; Whicher, A.; Camprubí, E.; Lane, N. The Origin of Life in Alkaline Hydrothermal Vents. *Astrobiology* **2016**, *16*, 181–197. [[CrossRef](#)] [[PubMed](#)]
52. Villafaña-Barajas, S.A.; Colín-García, M.; Negrón-Mendoza, A.; Ruiz-Bermejo, M. An experimental study of the thermolysis of hydrogen cyanide: The role of hydrothermal systems in chemical evolution. *Int. J. Astrobiol.* **2020**, 1–10. [[CrossRef](#)]
53. de la Fuente, J.L.; Ruiz-Bermejo, M.; Menor-Salván, C.; Osuna-Esteban, S. Thermal characterization of HCN polymers by TG–MS, TG, DTA and DSC methods. *Polym. Degrad. Stab.* **2011**, *96*, 943–948.
54. Fernández, A.; Ruiz-Bermejo, M.; de la Fuente, J.L. Modelling the kinetics and structural property evolution of a versatile reaction: Aqueous HCN polymerization. *Phys. Chem. Chem. Phys.* **2018**, *20*, 17353–17366.
55. Marín-Yaseli, M.R.; Moreno, M.; de la Fuente, J.L.; Briones, C.; Ruiz-Bermejo, M. Experimental conditions affecting the kinetics of aqueous HCN polymerization as revealed by UV–vis spectroscopy. *Spectrochim. Acta Part A* **2018**, *191*, 389–397.
56. Azamar, J.; Draganić, I. *Equipo para la preparación de compuestos tóxicos en solución acuosa y en atmósfera controlada: Cianuros para experimentos en Química de Radiaciones*; Informe Técnico Q5; Departamento de Química, CEN, UNAM: Mexico City, Mexico, 1982; p. 16.
57. Ferris, J.P.; Joshi, P.C.; Edelson, E.H.; Lawless, J.G. HCN: A plausible source of purines, pyrimidines and amino acids on the primitive earth. *J. Mol. Evol.* **1978**, *11*, 293–311. [[CrossRef](#)]
58. Colín-García, M.; Villafaña-Barajas, S.; Camprubí, A.; Ortega-Gutiérrez, F.; Colás, V.; Negrón-Mendoza, A. 5.4 Prebiotic Chemistry in Hydrothermal Vent Systems. In *Handbook of Astrobiology*; Kolb, V., Ed.; CRC Press: Boca Raton, FL, USA, 2018; pp. 297–329.
59. Matthews, C.N. Hydrogen cyanide polymers: From laboratory to space. *Planet. Space Sci.* **1995**, *43*, 1365–1370. [[CrossRef](#)]
60. Marín-Yaseli, M.R.; González-Toril, E.; Mompeán, C.; Ruiz-Bermejo, M. The Role of Aqueous Aerosols in the “Glyoxylate Scenario”: An Experimental Approach. *Chem. Eur. J.* **2016**, *22*, 12785–12799. [[CrossRef](#)]
61. Marín-Yaseli, M.R.; Cid, C.; Yagüe, A.I.; Ruiz-Bermejo, M. Detection of Macromolecular Fractions in HCN Polymers Using Electrophoretic and Ultrafiltration Techniques. *Chem. Biodivers.* **2017**, *14*, e1600241. [[CrossRef](#)] [[PubMed](#)]
62. Socrates, G. *Infrared and Raman Characteristic Group Frequencies: Tables and Charts*, 3rd ed.; Repr. as Paperback; Wiley: Chichester, UK, 2010; p. 366.
63. Schwartz, A.W.; Voet, A.B.; Veen, M. Recent progress in the prebiotic chemistry of HCN. *Orig. Life* **1984**, *14*, 91–98.
64. Minard, R.D.; Hatcher, P.G.; Gourley, R.C.; Matthews, C.N. Structural investigations of hydrogen cyanide polymers: New insights using TMAH thermochemolysis/GC-MS. *Orig. Life Evol. Biosph.* **1998**, *28*, 461–473.
65. Marín-Yaseli, M.R.; Mompeán, C.; Ruiz-Bermejo, M. A prebiotic synthesis of pterins. *Chem. Eur. J.* **2015**, *21*, 13531–13534. [[CrossRef](#)]
66. Borquez, E.; Cleaves, H.J.; Lazcano, A.; Miller, S.L. An investigation of prebiotic purine synthesis from the hydrolysis of HCN polymers. *Orig. Life Evol. Biosph.* **2005**, *35*, 79–90. [[CrossRef](#)]
67. Moser, R.E.; Claggett, A.R.; Matthews, C.N. Peptide formation from aminomalononitrile (HCN trimer). *Tetrahedron Lett.* **1968**, *9*, 1605–1608. [[CrossRef](#)]
68. Das, T.; Ghule, S.; Vanka, K. Insights into the origin of life: Did it begin from HCN and H₂O? *ACS Cent. Sci.* **2019**, *5*, 1532–1540. [[CrossRef](#)]
69. Toner, J.D.; Catling, D.C. Alkaline lake settings for concentrated prebiotic cyanide and the origin of life. *Geochim. Cosmochim. Acta* **2019**, *260*, 124–132. [[CrossRef](#)]
70. Smirnov, A.; Hausner, D.; Laffers, R.; Strongin, D.R.; Schoonen, M.A. Abiotic ammonium formation in the presence of Ni-Fe metals and alloys and its implications for the Hadean nitrogen cycle. *Geochem. Trans.* **2008**, *9*, 5. [[CrossRef](#)]
71. LaRowe, D.E.; Regnier, P. Thermodynamic potential for the abiotic synthesis of adenine, cytosine, guanine, thymine, uracil, ribose, and deoxyribose in hydrothermal systems. *Orig. Life Evol. Biosph.* **2008**, *38*, 383–397. [[CrossRef](#)]
72. Lupton, J.E.; Delaney, J.R.; Johnson, H.P.; Tivey, M.K. Entrainment and vertical transport of deep-ocean water by buoyant hydrothermal plumes. *Nature* **1985**, *316*, 621–623. [[CrossRef](#)]
73. Little, S.A.; Stolzenbach, K.D.; Von Herzen, R.P. Measurements of plume flow from a hydrothermal vent field. *J. Geophys. Res.* **1987**, *92*, 2587–2596. [[CrossRef](#)]

74. Bemis, K.; Lowell, R.; Farough, A. Diffuse Flow on and Around Hydrothermal Vents at Mid-Ocean Ridges. *Oceanography* **2012**, *25*, 182–191. [[CrossRef](#)]
75. Mittelstaedt, E.; Escartín, J.; Gracias, N.; Olive, J.-A.; Barreyre, T.; Davaille, A.; Cannat, M.; Garcia, R. Quantifying diffuse and discrete venting at the Tour Eiffel vent site, Lucky Strike hydrothermal field. *Geochem. Geophys. Geosyst.* **2012**, *13*, 1–18. [[CrossRef](#)]
76. Holm, N.G.; Hennem, R.J.-C. Hydrothermal systems: Their varieties, dynamics, and suitability for prebiotic chemistry. In *Marine Hydrothermal Systems and the Origin of Life*; Springer: Dordrecht, The Netherlands, 1992; pp. 15–31.
77. Allen, D.E.; Seyfried, W.E. Serpentinization and heat generation: Constraints from Lost City and Rainbow hydrothermal systems. *Geochim. Cosmochim. Acta* **2004**, *68*, 1347–1354. [[CrossRef](#)]
78. Yamaoka, K.; Kawahata, H.; Gupta, L.P.; Ito, M.; Masuda, H. Thermal stability of amino acids in siliceous ooze under alkaline hydrothermal conditions. *Org. Geochem.* **2007**, *38*, 1897–1909. [[CrossRef](#)]
79. Stüeken, E.E.; Anderson, R.E.; Bowman, J.S.; Brazelton, W.J.; Colangelo-Lillis, J.; Goldman, A.D.; Som, S.M.; Baross, J.A. Did life originate from a global chemical reactor? *Geobiology* **2013**, *11*, 101–126. [[CrossRef](#)]
80. Omran, A.; Pasek, M. A Constructive Way to Think about Different Hydrothermal Environments for the Origins of Life. *Life* **2020**, *10*, 36. [[CrossRef](#)]
81. Burcar, B.T.; Barge, L.M.; Trail, D.; Watson, E.B.; Russell, M.J.; McGown, L.B. RNA Oligomerization in Laboratory Analogues of Alkaline Hydrothermal Vent Systems. *Astrobiology* **2015**, *15*, 509–522. [[CrossRef](#)]
82. Mompeán, C.; Marín-Yaseli, M.R.; Espigares, P.; González-Toril, E.; Zorzano, M.-P.; Ruiz-Bermejo, M. Prebiotic chemistry in neutral/reduced-alkaline gas-liquid interfaces. *Sci. Rep.* **2019**, *9*, 1–12. [[CrossRef](#)]
83. Holm, N.G.; Dumont, M.; Ivarsson, M.; Konn, C. Alkaline fluid circulation in ultramafic rocks and formation of nucleotide constituents: A hypothesis. *Geochem. Trans.* **2006**, *7*, 7. [[CrossRef](#)] [[PubMed](#)]



© 2020 by the authors. Licensee MDPI, Basel, Switzerland. This article is an open access article distributed under the terms and conditions of the Creative Commons Attribution (CC BY) license (<http://creativecommons.org/licenses/by/4.0/>).